Structural Durability & Health Monitoring
DOI:10.32604/sdhm.2020.08792
Article

Finite Element Model Updating for Structural Health Monitoring

Amirabbas Haidarpour and Kong Fah Tee*

School of Engineering, University of Greenwich, Chatham Maritime, Kent, ME4 4TB, UK
*Corresponding Author: Kong Fah Tee. Email: K.F.Tee@gre.ac.uk
Received: 09 October 2019; Accepted: 19 December 2019

Abstract: This paper provides a model updating approach to detect, locate, and characterize damage in structural and mechanical systems by examining changes in measured vibration responses. Research in vibration-based damage identification has been rapidly expanding over the last few decades. The basic idea behind this technology is that modal parameters (notably frequencies, mode shapes, and modal damping) are functions of the physical properties of the structure (mass, damping, and stiffness). Therefore, changes in the physical properties will cause changes in the modal properties which could be obtained by structural health monitoring (SHM). Updating is a process fraught with numerical difficulties. These arise from inaccuracy in the model and imprecision and lack of information in the measurements, mainly taken place in joints and critical points. The motivation for the development of this technology is presented, methods are categorized according to various criteria such as the level of damage detection provided from vibration testing, natural frequency and mode shape readings are then obtained by using modal analysis techniques, which are used for updating structural parameters of the associated finite element model. The experimental studies for the laboratory tested bridge model show that the proposed model updating using ME'scope technique can provide reasonable model updating results.

Keywords: Structural health monitoring; model updating; natural frequency; mode shape; stiffness; vibration testing

1 Introduction

The interest in the ability to monitor a structure and detect damage at the earliest possible stage is very important throughout the civil, mechanical, and aerospace engineering communities and it will prevent from any mitigation action and human lost, as well as financial loses [1, 2]. For the purposes of this paper, damage is defined as changes introduced into a system, which affect the structure performance [3]. Structural health monitoring (SHM) is a term includes wide range of methods and practices which aim to assess condition of a structure based on combination of observation, measurement, analysis, and modelling [4].

The size and complexity of civil infrastructures demands global methods for evaluating their performance and condition. Such a strategy requires lots of sensors distributed throughout the structure to identify the damage [5]. The technology developed measures structural response giving more support in the structural design and construction. Local methods are very specified and advanced, and it will give most possible indication to the damaged locations, obviously such a technique, it will be time consuming as well as more challenging [6]. Needs for effective SHM has become increasingly important in recent

years. At the early stage in civil infrastructure health monitoring, visual inspection was more in practice. Vibration-based methods have been developed for the last two decades [7, 8].

The need for quantitative global damage detection methods that can be applied to complex structures has led to the development and continued research of methods that examine changes in the vibration characteristics of the structure [9]. Structural damage identification techniques based on vibration measurements show great promises because they allow for quick and global damage detection at a relatively low cost after a severe loading event. These techniques rely on the fact that any change in stiffness caused by damage in a structure leads to a change in modal parameters of the structure such as frequencies and mode shapes [10]. Although successful applications of these techniques have been developed to some extent, vibration based local damage assessment of bridges remains a challenge in practice.

The methods are categorized according to various criteria such as the level of damage detection provided, model-based *vs*. non-model-based methods and linear *vs*. nonlinear methods [11]. The existing methods for damage identification using measured vibration modal data include model updating techniques, sensitivity analysis methods and dynamic perturbation methods. However, most of these methods may be unable to provide accurate predictions for the severity of damage at specific locations in complex structures such as bridges because the chosen damage indicators are not capable of reflecting the severity of the damage at local level. The process of implementing a damage identification of structures is a continuous process of SHM, as a part of it, vibration-based damage detection brings more attention of many researchers [12-14].

Finite element (FE) procedures for structural analysis within practical applications often expose considerable discrepancy between analytical prediction and experimental test results [15-17]. To reduce discrepancy, it is required to modify the modelling assumptions and parameters until the link between analytical predictions and experimental test results satisfies the requirements. To adjusting parameters of the finite element model, experimental test is required too, as the FE numerical model of a physical structure may not cover all the physical and geometrical aspects of the actually built structure. Characteristically, this will be achieved by a trial and error approach, which could be time consuming and may not be sensible in some cases. Hence a computational procedure has been developed to update the parameters of analytical models using test data. Model updating methods using vibration measurements mainly has two types: response based methods and modal based methods [18-20]. In response based methods, the measured frequency response function (FRF) data are intended for updating FE numerical models. Structural parameters such as stiffness and mass are identified often by minimising a residual error between FE numerical and experimental results [21-23].

Another type of FE model updating methods is modal based methods, where modal data, such as natural frequencies and mode shapes, are utilised in the structural parameter updating process. The modal based methods update structural parameters of the FE model often by an optimisation process, which requires the eigen solutions and associated sensitivity matrices of the FE model. The performance of the modal based methods mainly depends on optimisation techniques and requires significant computational hard work in the model updating process [24]. The objective function can be taken as the residuals between the measured modal data and the corresponding predictions from the initial FE model, such as difference in frequencies and mode shape measurements.

This paper presents an effective approach for monitoring the overall health of structures using finite element analysis and ME'scope for updating. Experimental testing is conducted to identify the bridge structural parameters and modal parameters using the collected vibration data. Finite element results will be discussed and compared with experimental testing to assess bridge condition and detect damage using the vibration-based technique. The paper will also serve in developing a tool that can be used for long term bridge performance assessment.

2 Experimental Testing

A scale down space frame prototype steel bridge truss structure as shown in Fig. 1 was built for the laboratory vibration testing to demonstrate the effectiveness of the proposed FE model updating method.

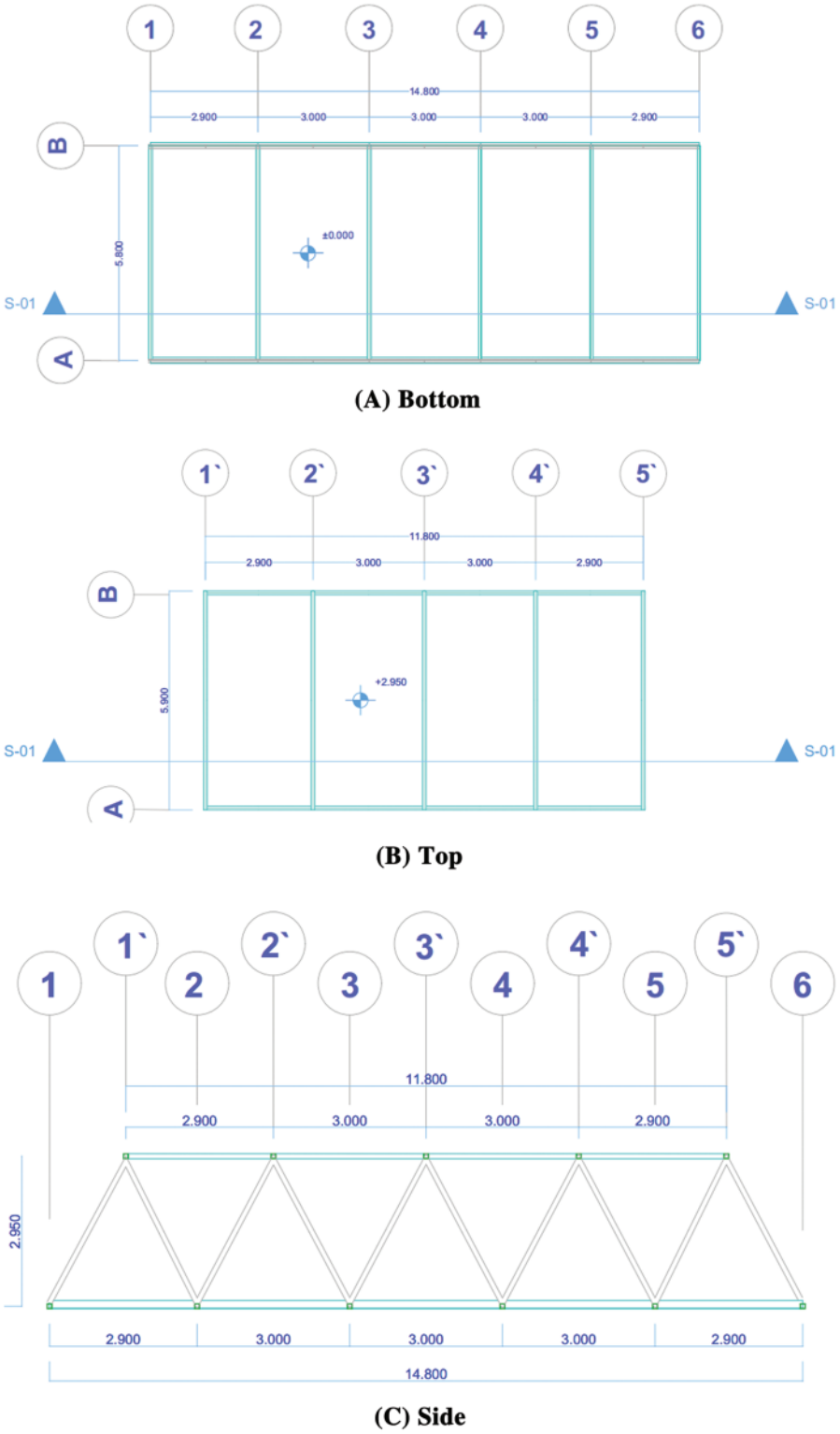

Figure 1: Engineering drawing of the tested truss bridge. (A) Bottom, (B) Top, and (C) Side

The structure was fixed into a steel base frame. The structure was constructed by two continuous steel members at the bottom with an L shape section of dimensions of 16 mm (length) by 3 mm (thickness), and two top steel members with a solid square section of dimensions of 10 mm by 10 mm. The remaining elements were welded to the associated top and bottom members to form a space bridge model structure. The structure was 1480 mm long in total, 570 mm wide and 290 mm high. The spacing between two diagonal links was 300 mm. In the laboratory vibration testing for the bridge model, a total number of 18 accelerometers were placed at joints to measure translational displacement. Two types of uniaxial sensors (i.e., PCB 353B33 and 353B32) were used in testing and installed at joints to record the response of the bridge model structure excited by impulse hammer. The dynamic response data were acquired by using five DAQ signal processing modules with 4-channel 24-Bit AC/DC input module and a data acquisition chassis, and then collected by LabVIEW signal processing software. Bridge model structure and equipments used in laboratory for structural dynamic testing shown in Fig. 2.

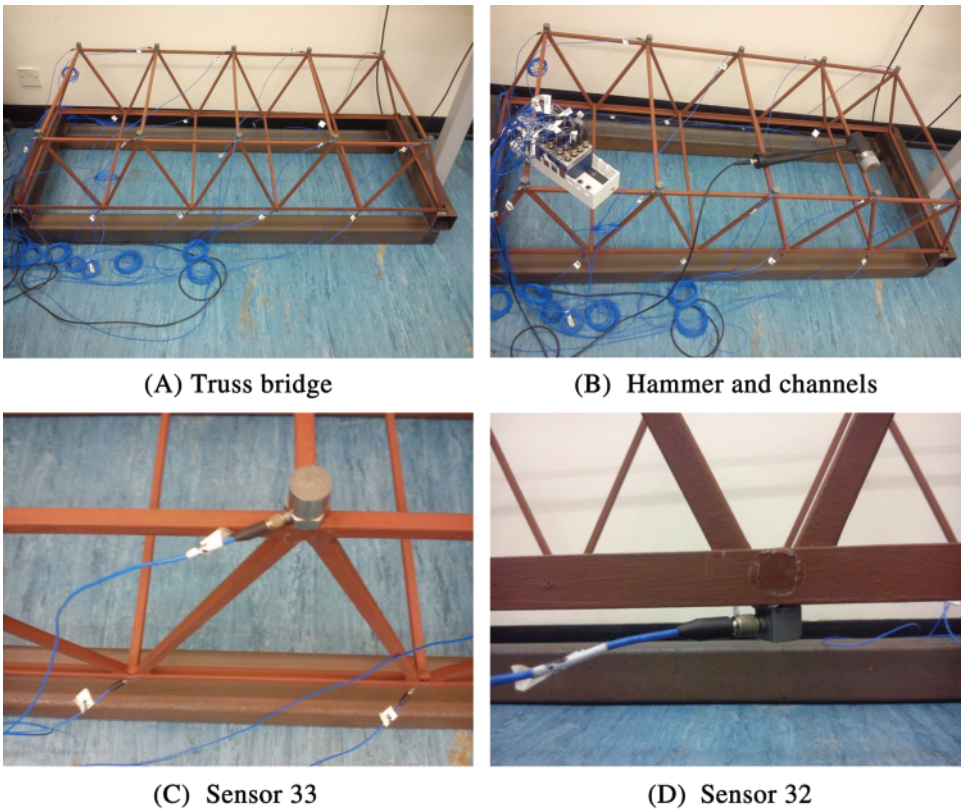

Figure 2: Bridge model structure and equipments used in laboratory for structural dynamic testing. (A) Truss bridge, (B) Hammer and channels, (C) Sensor 33, and (D) Sensor 32

Accelerometers were then connected by low noise cable (model 003C20) to the input module. PCB model 086D20 impact hammer mounted transducer was used to excite the structure at specified locations. A super soft rubber hammer tip (model 084A60) was attached in the hammer to broaden the impulse that was passed on to structure in an effort to better excite the lower frequency modes.

Sensors are being used and sensor connected to sensor detecting device (amplifier) to receive the signals from sensors, which had connected to the structure at required points or nodes. The amplifier sends the data to

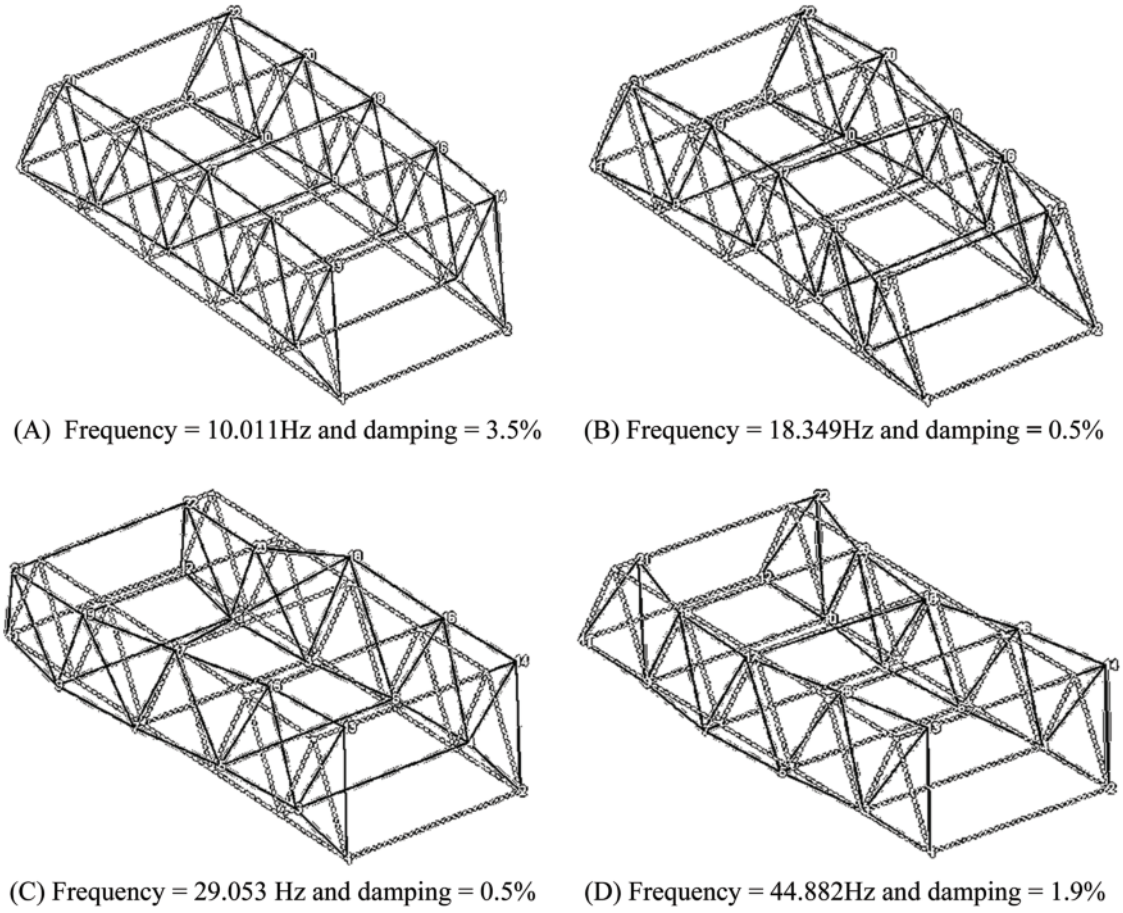

Figure 3: First four identified modes of truss bridge: (A) Mode 1: Frequency = 10.011 Hz and damping = 3.5%, (B) Mode 2: Frequency = 18.349 Hz and damping = 0.5%, (C) Mode 3: Frequency = 29.053 Hz and damping = 0.5%, and (D) Mode 4: Frequency = 44.882 Hz and damping = 1.9%

the personal computer and the data obtained from the signal receiver has been converted into the required format for extracting vibration parameters of structures such as frequency and mode shape (Fig. 3) of all nodes at different loading conditions on that structure. Tab. 1 shows the direction of each sensor and experimental results for the first 8 modes.

Figure 4 visualises acceleration in time domain and frequency domain (as power spectral density) at node 16 in the X-direction. Fig. 5 shows the maximum level of frequency extracted from the test. The average of the power spectral density of the selected channel is calculated. The principal angle plot as shown in Fig. 6 shows clearly the gap, which indicates that the real model order is situated. In theory, higher orders will not provide better results. For real-life measurements, this gap will never be that obvious, but in some cases, it will help to define approximately the model order of the measured structure. Fig. 7 shows that since there is a high number of stable poles (the blue circles), the stabilization criteria can be made a little more stringent. Only the most stable poles are shown. Fig. 8 shows structural response in frequency domain with magnitude data within a limited range of frequency (0–140 Hz).

Table 1: Directions of each sensor, as well as mode shapes, frequencies and damping

		Mode	1	2	3	4	5	6	7	8
		Frequency	10.011	18.349	29.053	44.882	53.76	72.875	101.82	107.16
		Damping	4.9516	4.6871	1.3754	5.3228	1.8031	2.7624	0.0662	0.23489
Node		Direction DOF								
3	−180	X-Direction	−0.62109	0.21789	0.44759	0.53384	0.15777	0.5517	0.85395	0.31271
4	0	X-Direction	0.53267	−0.1765	−0.3821	−0.50913	−0.1659	−0.5395	−0.927	−0.3081
5	−180	X-Direction	−0.81315	0.81762	0.17409	0.74111	−0.0903	0.2078	−0.3579	−0.25
6	0	X-Direction	0.7889	−0.8421	−0.1917	−0.7284	0.08906	−0.2383	0.36869	0.22251
7	−180	X-Direction	−0.76581	1	−0.2607	0.67096	−0.7562	−0.2071	−0.7753	−0.259
8	0	X-Direction	0.76858	−0.9982	0.3423	−0.60779	0.72009	0.1473	0.73624	0.29773
9	−180	X-Direction	−0.54249	0.56582	−0.4467	0.68494	−0.8192	−0.5689	1	0.38834
10	0	X-Direction	0.50035	−0.5549	0.45897	−0.64586	0.79285	0.5252	−0.9416	−0.4864
13	−180	X-Direction	−0.76746	−0.5094	0.92104	0.03677	−0.99	0.5489	−0.6908	0.21215
14	0	X-Direction	0.7394	0.4939	−0.868	−0.03576	1	−0.5725	0.37992	−0.193
15	−180	X-Direction	−0.93853	0.20753	0.67206	−0.14631	0.24665	−0.9839	0.2879	−0.3598
16	0	X-Direction	0.94682	−0.2043	−0.6995	0.15106	−0.2577	1	−0.0373	0.62764
17	−180	X-Direction	−0.99086	0.67438	−0.0782	−0.80173	0.84979	−0.1078	0.40694	1
18	0	X-Direction	1	−0.6884	0.00746	0.81273	−0.8733	0.118	−0.4754	−0.6656
19	−180	X-Direction	−0.87119	0.70743	−0.6977	−0.98149	0.27479	0.965	−0.2994	−0.5115
20	0	X-Direction	0.88518	−0.7428	0.73303	1	−0.2799	−0.9841	0.31821	0.41732
21	−180	X-Direction	−0.59162	0.2837	−0.678	−0.36611	−0.0136	−0.4989	−0.1089	0.20585
22	0	X-Direction	0.58596	−0.2887	0.6784	0.36526	0.03459	0.4348	0.05402	−0.1324
18	90	Z-Direction	−0.0608	−0.3637	1	0.03196	−0.0268	−0.0384	−0.0114	−0.2681

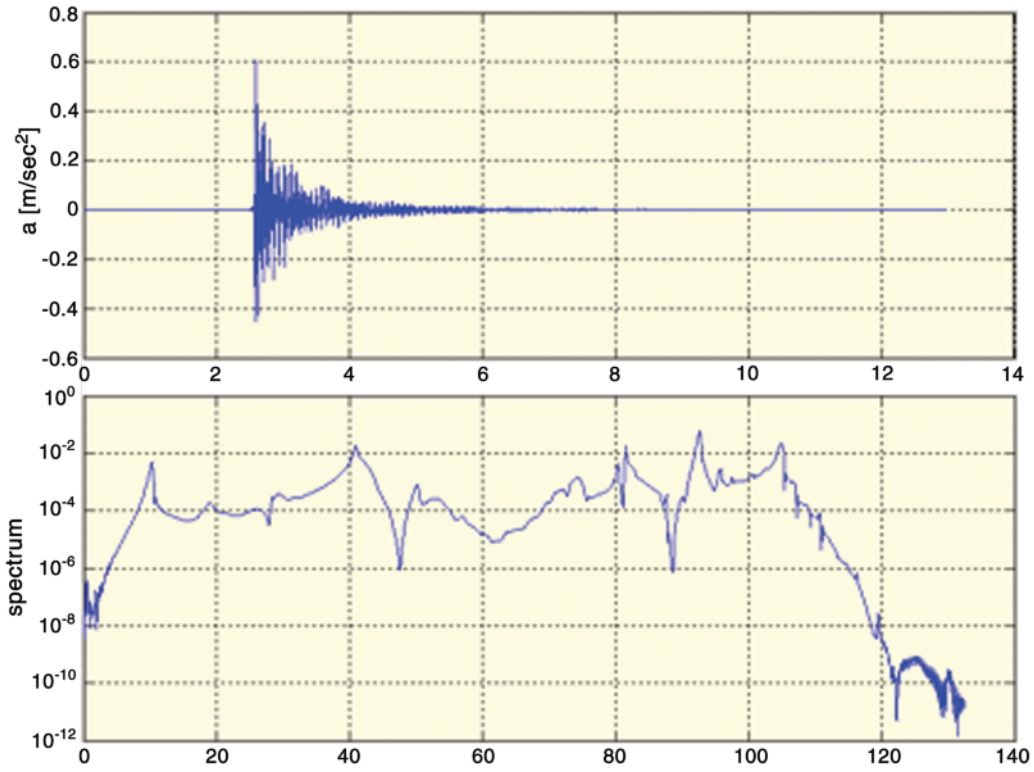

Figure 4: Visualization window for acceleration with time domain and frequency domain

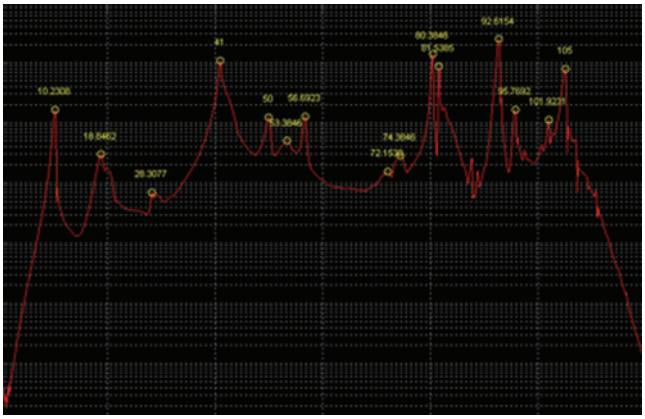

Figure 5: Frequency at pick points

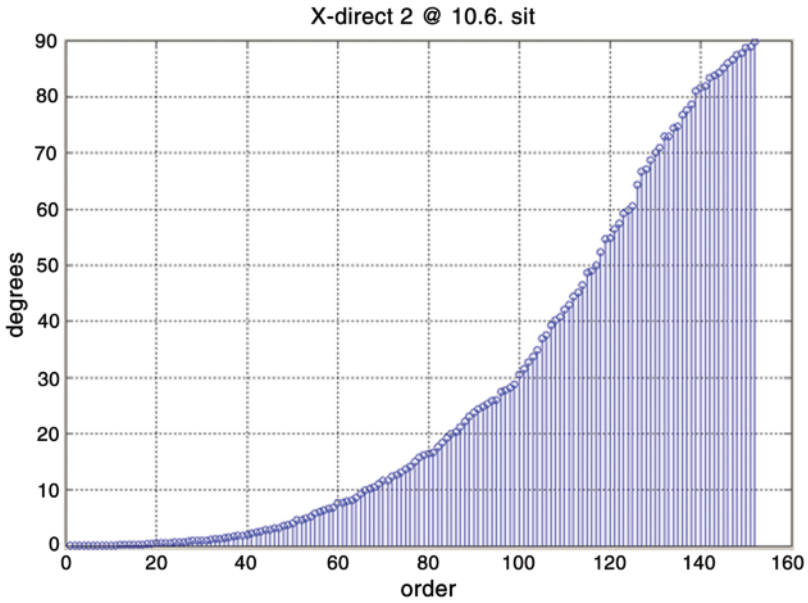

Figure 6: Principle angle compares to the degrees of order

3 Finite Element Analysis

The finite element structure is identical to that used in experiments. The load is applied in an identical fashion to experiments, i.e., through hammer loading. The finite element simulation created in ANSYS has modelled the main frame which is made up of two main beams with L-shape at the bottom of the frame and bracings to resist lateral forces. The specification of the truss bridge model is shown in Fig. 1. The finite element model of the laboratory prototype structure illustrating the geometric dimensions, nodes and elements are shown in Fig. 9. The bracings are all presumed to be pin-jointed at two ends. The connection joint of the main frame is modelled as rigid connection to withstand bending moments. The finite element model has 22 nodes and 49 elements with an overall 114 degrees of freedom (DOFs). The two beams at the bottom of the tested bridge model which form part of the main frame have L-shape cross section with dimension of 16 mm × 16 mm × 3 mm, while the remaining part of the main frame and the bracings have a square cross-section with dimension of 10 mm × 10 mm.

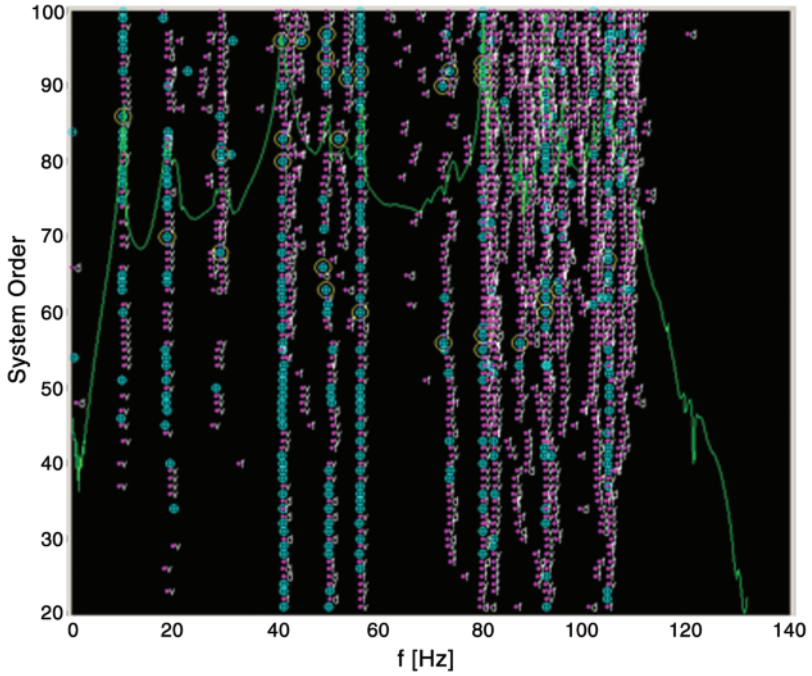

Figure 7: Stabilisation diagram indicating natural frequency measurements

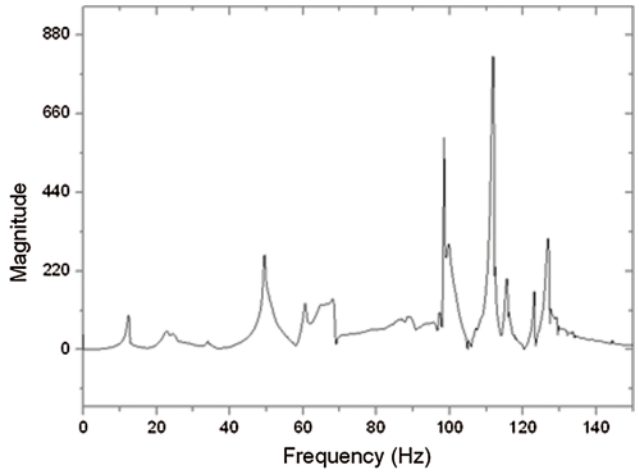

Figure 8: Structural response in frequency domain with magnitude data *vs*. frequency

The component of the prototype bridge structure is steel. The structure is comprised of two units: the frame and the bracings. The frame is modelled using BEAM188 and the bracings are modelled using LINK180, respectively. The advantage of BEAM188 is that it is a uniaxial element that has torsion, tension, and compression, and also has bending abilities. BEAM188 element has six DOFs at each node namely translations in x, y and z nodal directions, and rotations in the x, y and z nodal directions. Also, LINK180 element is a two-dimensional element with uniaxial tension and compression element. It has only two DOFs at each node namely translations in the x and y nodal directions. For LINK180 element, the real constant is defined with a cross-sectional area of 1.0×10^{-4} m^2.

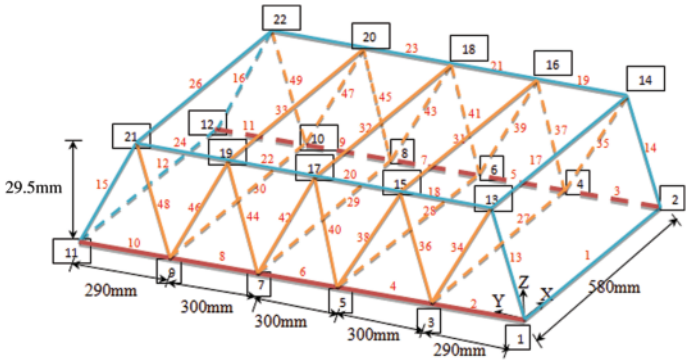

Figure 9: Test structure details

The element material properties of the tested truss bridge structure are defined as elastic and isotropic, Young's Modulus = 200 GPa, Poison's Ratio = 0.30, and density = 7850 kg/m^3. Each element in the bridge frame has two nodes; therefore, the elements are created by joining nodes. Boundary conditions are assigned to nodes 1, 2, 11 and 12. At nodes 1 and 2, the nodes are fixed. While at nodes 11 and 12, translations are restrained in x and z directions and rotations are allowed in all directions.

The objective of this analysis is to evaluate and update the experimental model using finite element results. Simulations are based on different conditions of the structure. When the structure has been damaged, there are some changes in natural frequencies and mode shapes due to reductions in stiffness. Four different scenarios have been studied as shown in Fig. 10. Case A is the healthy condition in which the mode shapes and frequencies are extracted and compared with damaged situations. Case B is a damaged condition with damaged element connects nodes 6 to 18. In this situation because the damaged element is one of the links, it does not have huge impact in mode shapes and frequencies in comparison to the original case. Case C is a damaged condition with damaged element connects nodes 14 to 16. In this scenario once again the damage element is one of the links, it does not have huge impact in mode shapes and frequencies in comparison to the original case. Similar to Case B, the damaged element is not a very critical point and damage itself is not severe too (Young modulus drops from 2e11 to 2e5).

Case D is a damaged condition with damaged element connects nodes 6 to 8. In this situation because the damaged element is a critical part of the structure and it is a frame element, it has huge impact in mode shapes and frequencies in comparison to the original case as illustrated in Fig. 11. Although Cases B, C and D have the same reduction of Young modulus, the changes of frequencies are different depending on the location of the damaged element. Modal analysis is performed for the tested bridge model to determine the frequencies and mode shapes. The result of frequencies is given in Tab. 2 and the mode shapes are presented in Figs. 12, 13, 14 and 15 for four Cases A, B, C and D.

ANSYS is used to obtain displacement vectors and rotational vectors for each mode. The displacement vectors (Ux, Uy, Uz) and rotational vectors (Rx, Ry, Rz) for required for the first 10 mode shapes at every node. Tab. 3 shows that nodal solution with displacement in x, y, z directions (Ux, Uy, Uz) and also maximum absolute values for node 18 in the x direction, node 12 in the y direction and node 18 in the z direction. To extract the best result from the experimental test, sensors are placed in 3 directions to identify displacement in all directions for optimising the best result [25]. However, impact load has massive influence in regard to sensors directions. Moreover, when there is a damaged element, there will have impact in structural strength. This is in relationship with stiffness and normally mass will not be considered unless there is a massive mass loss which is going to be very dangerous and should be

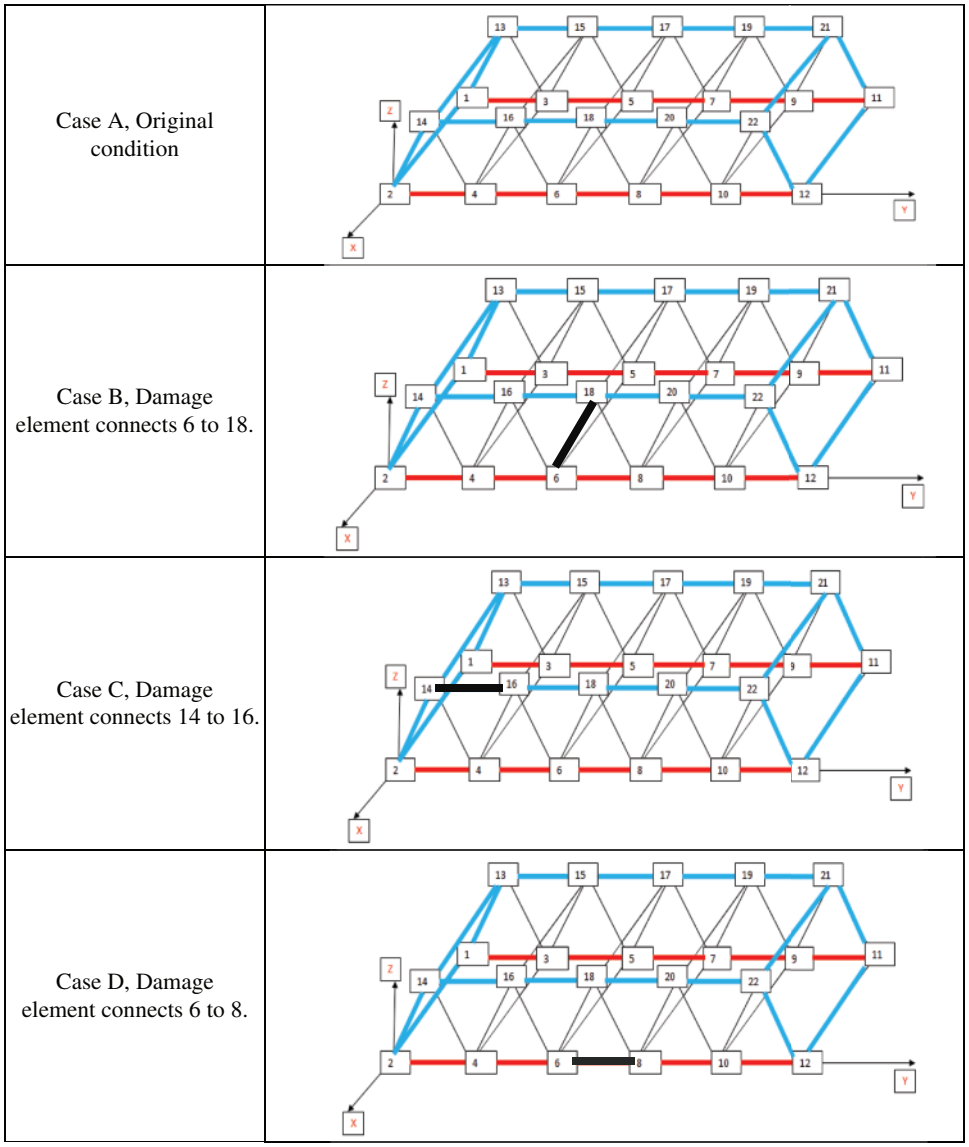

Figure 10: Damages Cases presented with black lines

monitored right away. Maintenance should be carried out to make sure structure is safe to be used or in case of severe defect, repair should be done.

4 Comparison between Finite Element Analysis and Lab Test

This technique identifies the state space matrices on the basis of the measurements by using robust numerical techniques, such as singular value decomposition. Once the mathematical description of the structure (truss bridge model) has been determined, it is straightforward to extract natural frequencies from the stabilisation diagram, and also to produce the associated mode shapes. Comparisons between lab test and numerical result have been completed to ensure extracted data are reliable, using MAC files; The function of the modal assurance criterion (MAC) is to provide a measure of consistency (degree of linearity) between lab test and finite element modal vector as shown in Tab. 4.

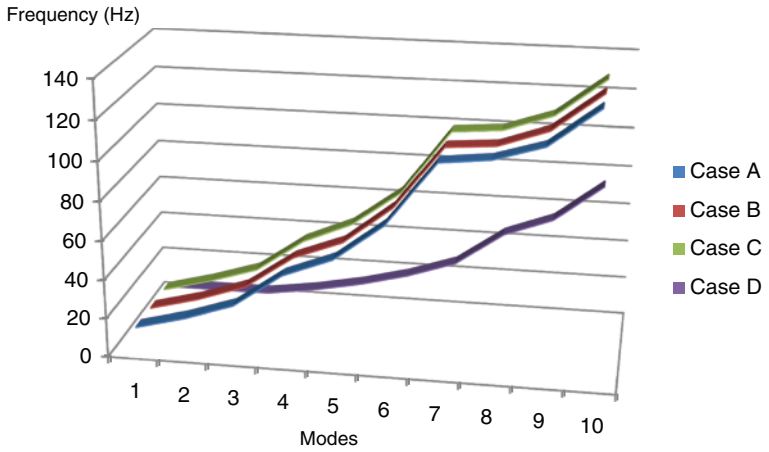

Figure 11: Frequencies for Cases A, B, C and D

Table 2: Frequencies for the first 10 modes for Cases A, B, C and D

Mode/Freq (Hz)	Case A	Case B	Case C	Case D
1	13.306	13.092	13.197	4.7934
2	19.733	19.551	19.694	4.8055
3	28.053	28.024	27.496	4.858
4	45.451	45.07	44.57	8.4679
5	55.108	54.597	55.088	13.305
6	73.847	73.832	73.079	19.653
7	106.1	105.8	105.98	28.051
8	108.77	107.71	108.01	45.45
9	116.37	116.37	116.37	54.768
10	135.49	135.48	135.48	73.847

This provides an additional confidence factor in the evaluation of a modal vector from different excitation (reference) locations or different modal parameter estimation algorithms. The modal scale factor and the modal assurance criterion (MAC) also provide a method of comparing modal vectors originating from different sources. The modal vectors from a finite element analysis can be compared and contrasted with those determined experimentally as well as modal vectors determined by different experimental or modal parameter estimation methods.

The modal assurance criterion takes on values from zero, representing no consistent correspondence, to one, representing a consistent correspondence. In this manner, if the modal vectors under consideration truly exhibit a consistent, linear relationship, the modal assurance criterion should approach unity and the value of the modal scale factor can be considered to be reasonable, as shown in Fig. 16. The modal assurance criterion can only indicate consistency, not validity or orthogonality. Invalid assumptions are normally the cause of this sort of potential error. Even though the modal assurance criterion is unity, the assumptions involving the system or the modal parameter estimation techniques are not necessarily correct.

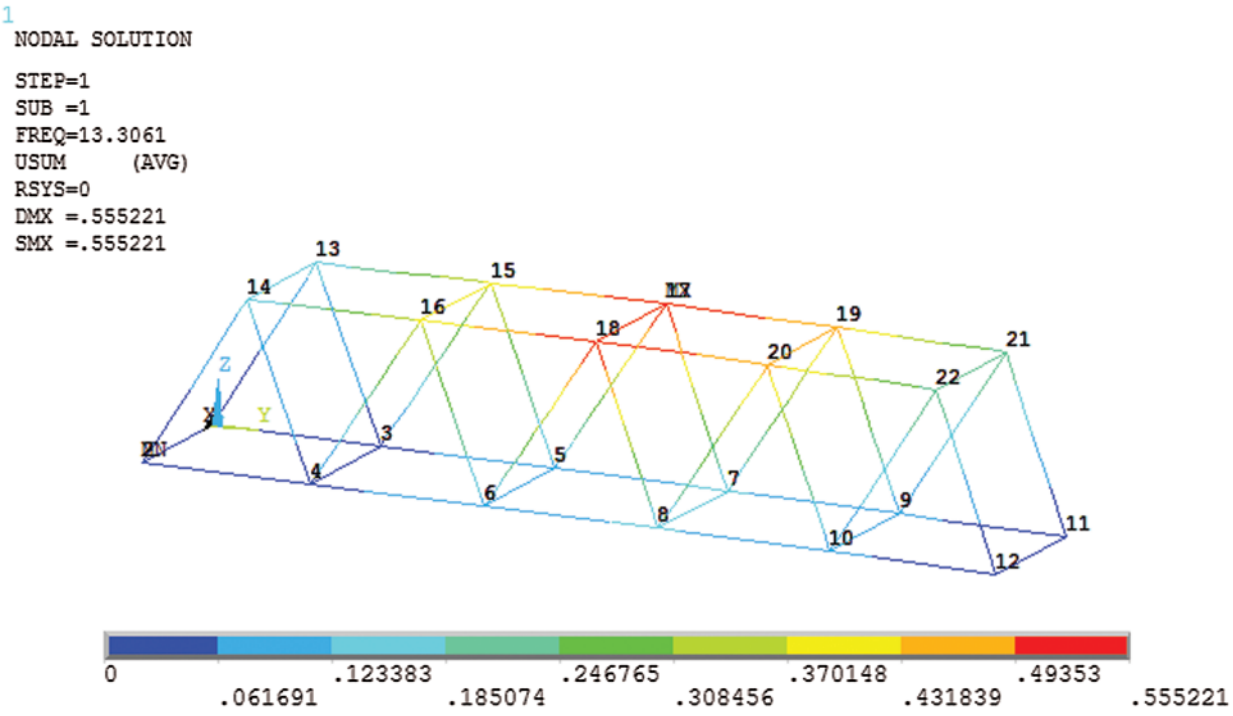

Figure 12: Case A: Numerical mode shapes and frequencies (Young modulus 2e11 Pa)

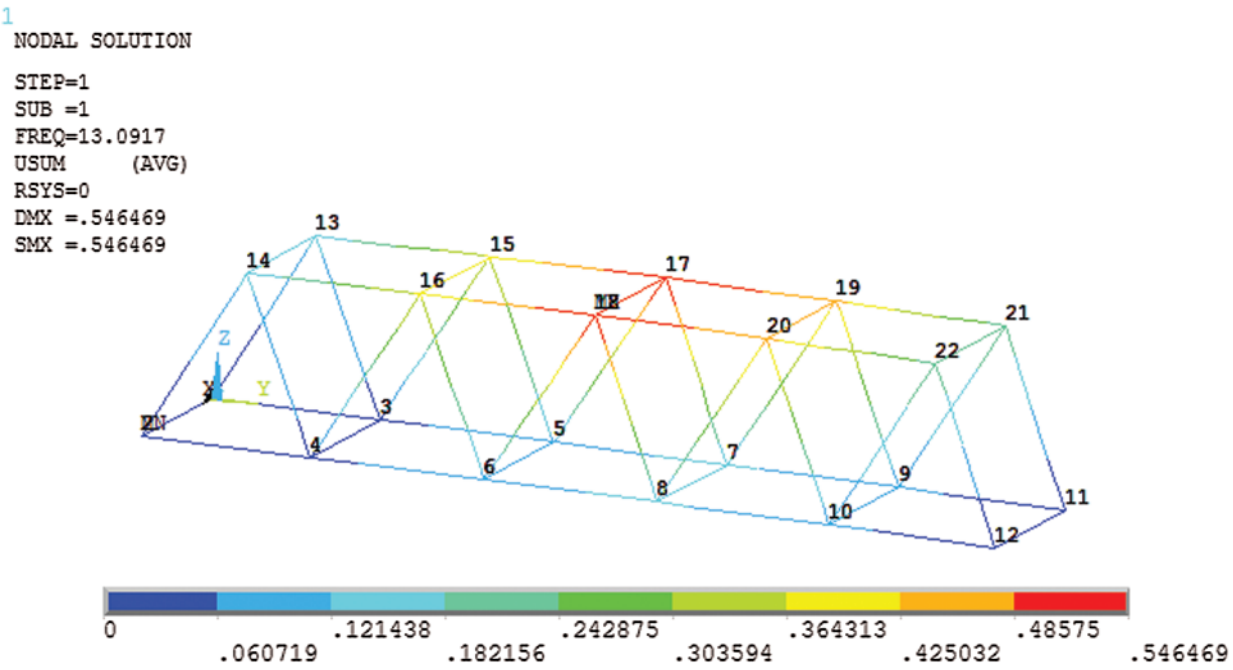

Figure 13: Case B: Numerical mode shapes and frequencies (Young modulus 2e5)

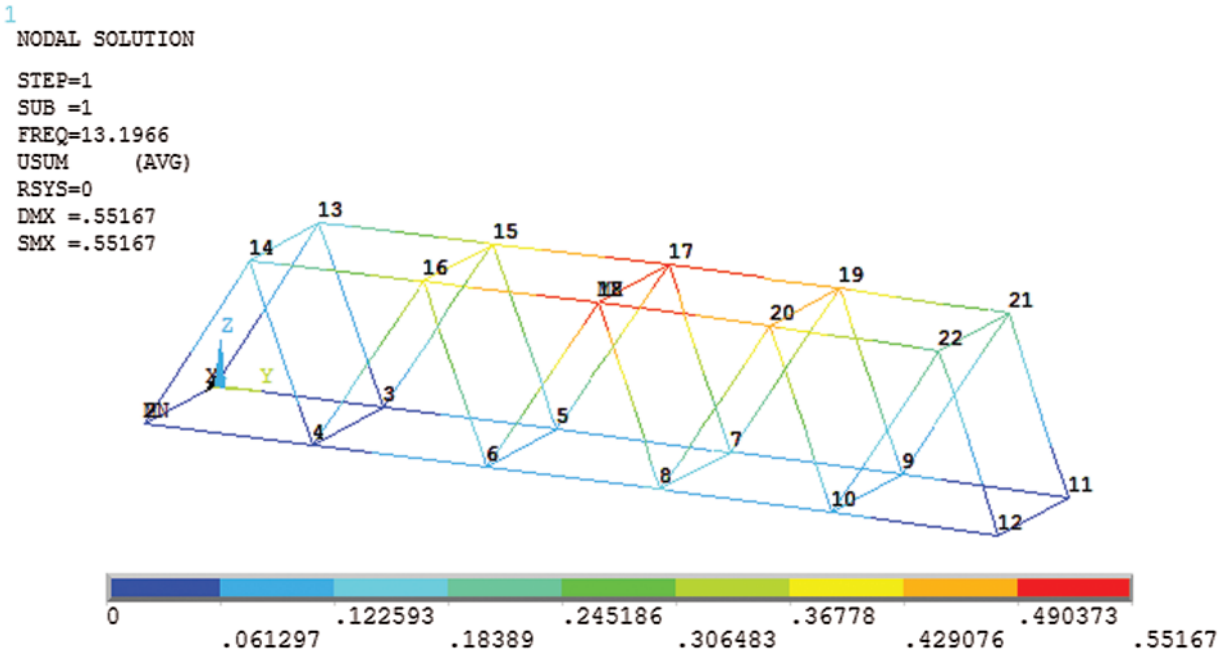

Figure 14: Case C: Numerical mode shapes and frequencies (Young modulus 2e5 Pa)

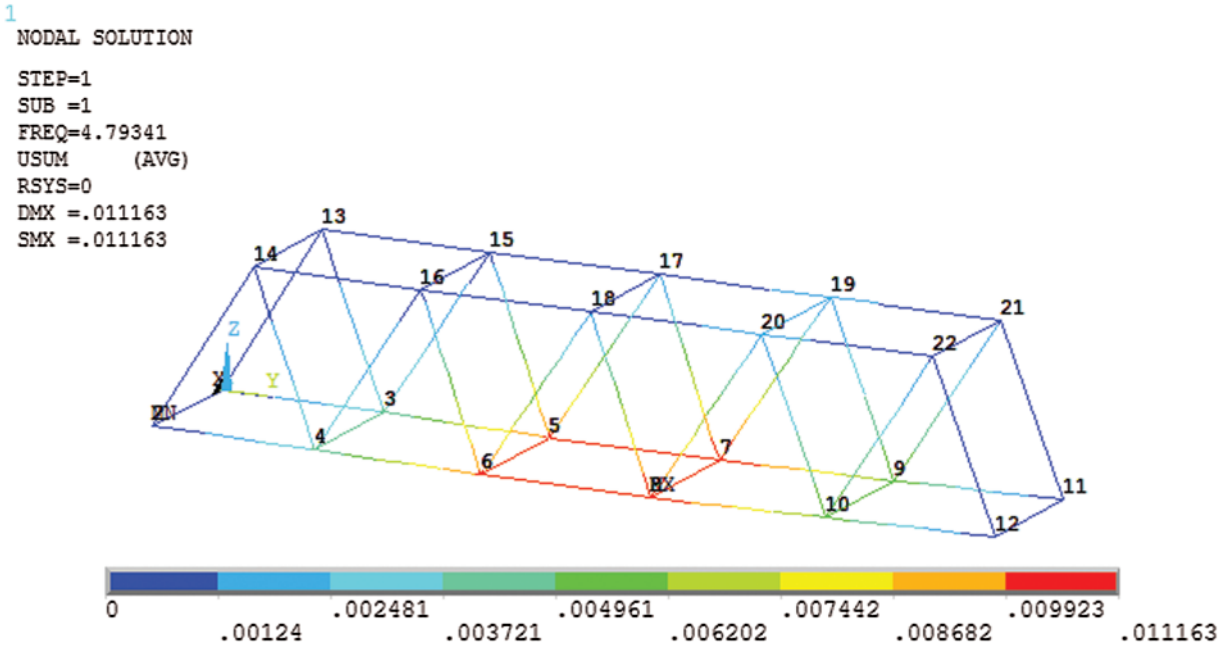

Figure 15: Case D: Numerical mode shapes and frequencies (Young modulus 2e5 Pa)

Table 3: Nodal solution displacement in x, y, z directions for Mode 1 in Case A

Node	UX	UY	UZ	USUM
1	0	0	0	0
2	0	0	0	0
3	−4.10E-02	4.49E-05	−1.27E-04	4.10E-02
4	−4.10E-02	−4.49E-05	1.27E-04	4.10E-02
5	−0.10775	1.01E-04	−1.92E-04	0.10775
6	−0.10775	−1.01E-04	1.92E-04	0.10775
7	−0.12933	1.61E-04	−1.97E-04	0.12933
8	−0.12933	−1.61E-04	1.97E-04	0.12933
9	−8.23E-02	2.18E-04	−1.33E-04	8.23E-02
10	−0.82260E	−1.00022	1.33E-04	8.23E-02
11	0	2.64E-04	0	2.64E-04
12	0	−2.64E-04	0	2.64E-04
13	−0.1342	9.64E-05	−8.86E-05	0.1342
14	−0.1342	−9.64E-05	8.86E-05	1.34E-01
15	−0.37849	1.18E-04	−1.74E- 04	0.37849
16	−0.37849	−1.18E-04	1.74E-04	0.37849
17	−0.55522	1.33E-04	−2.10E-04	0.55522
18	−0.55522	−1.33E-04	2.10E-04	0.55522
19	−0.44891	1.47E-04	−1.80E-04	0.44891
20	−0.44891	−1.47E-04	1.80E-04	0.44891
21	−0.22259	1.69E-04	−9.54E-05	0.22259
22	−0.22259	−1.69E-04	9.54E-05	0.22259
Maximum Absolute Values				
Node	18	12	18	18
Value	−0.55522	−2.64E-04	2.10E-04	0.55522

Table 4: Modal Assurance Criterion (MAC)

		Experimental results					
	Frequency, Hz	10.01	18.35	29.53	44.88	53.76	72.87
Numerical results	13.30	0.991000	0.006620	0.271000	0.000367	0.006450	0.001510
	19.73	0.006530	0.991000	0.002380	0.267000	0.000311	0.013400
	28.05	0.270000	0.002380	0.995000	0.000018	0.480000	0.000151
	45.45	0.000378	0.266000	0.000016	0.992000	0.000627	0.655000
	55.11	0.006420	0.000272	0.479000	0.000632	0.995000	0.000434
	73.85	0.001490	0.013400	0.000150	0.655000	0.000428	0.992000

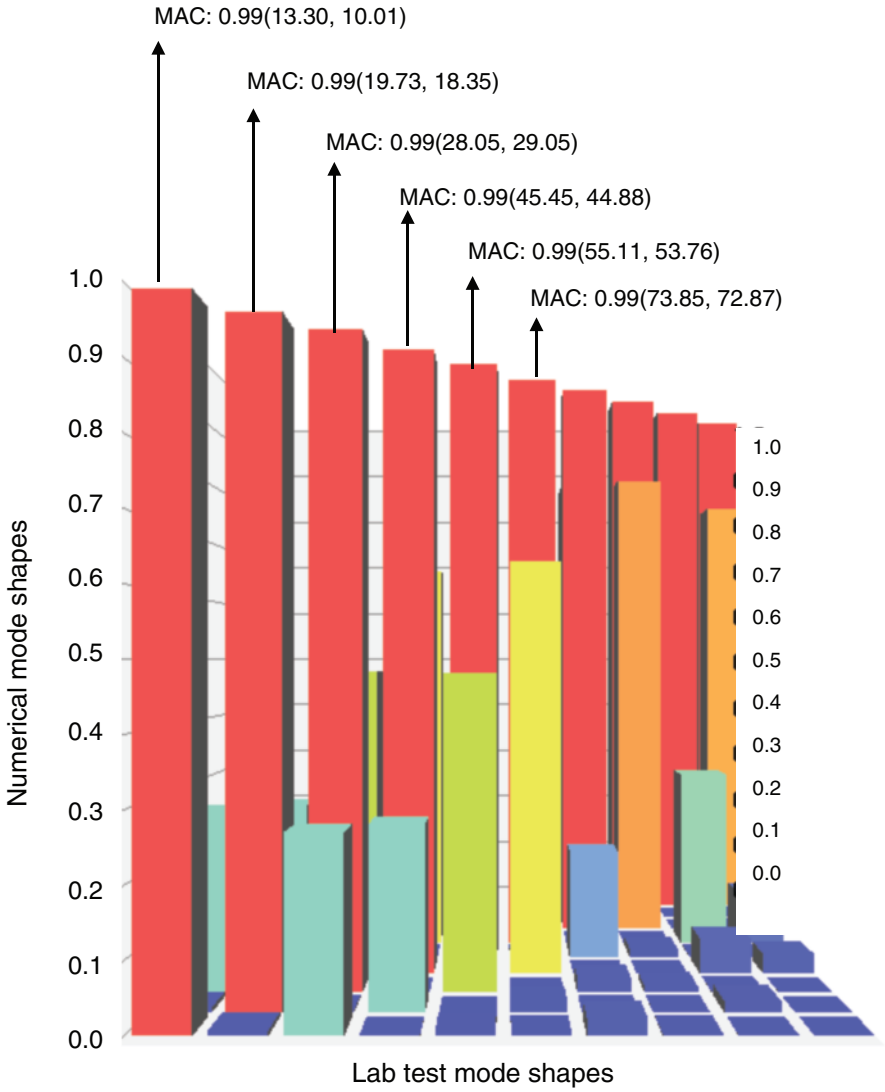

Figure 16: Undamaged numerical bridge model mode shape *vs*. lab test mode shape

5 Conclusions

The physical model of truss bridge structure was used for the experimental test to investigate its structural health condition by extracting the model parameters. The laboratory dynamic testing was undertaken for the constructed steel bridge model structure. Modal data such as frequencies and mode shape were obtained through the modal identification technique. The laboratory tested bridge model structure was then utilised to demonstrate the effectiveness of the proposed methods for updating the FE model by experimental studies. The proposed approach is capable of structural health monitoring and any changes in the structural condition have a direct impact in structural parameters such as stiffness as shown in numerical results.

Funding Statement: The author(s) received no specific funding for this study.

Conflicts of Interest: The authors declare that they have no conflicts of interest to report regarding the present study.

References

1. Zhang, Y., Kim, C. W., Tee, K. F., Garg, A., Garg, A. (2018). Long-term health monitoring for deteriorated bridge structures based on copula theory. *Smart Structures and Systems, 21(2),* 171–185.
2. Brownjohn, J. M. W., Xia, P. Q. (2000). Dynamic assessment of curved cable-stayed bridge by model updating. *Journal of Structural Engineering, 126(2),* 252–260. DOI 10.1061/(ASCE)0733-9445(2000)126:2(252).
3. Tee, K. F. (2019). Chapter 6: optimization of condensed stiffness matrices for structural health monitoring. In: Belgasmia, M., (eds.) *Optimization of Design for Better Structural Capacity*. Hershey, PA: IGI Global, 150–185.
4. Koh, C. G., Quek, S. T., Tee, K. F. (2002). Damage identification of structural dynamic system. *Proceedings of the 2nd International Conference on Structural Stability and Dynamics, Singapore*, 780–785.
5. Alvandi, A., Cremona, C. (2006). Assessment of vibration-based damage identification techniques. *Journal of Sound and Vibration, 292(1-2),* 179–202. DOI 10.1016/j.jsv.2005.07.036.
6. Pandey, A., Biswas, M., Samman, M. (1991). Damage detection from changes in curvature mode shapes. *Journal of Sound and Vibration, 145(2),* 321–332. DOI 10.1016/0022-460X(91)90595-B.
7. Tee, K. F. (2018). Time series analysis for vibration-based structural health monitoring: a review. *Structural Durability and Health Monitoring, 12(3),* 129–147.
8. Zou, Y., Tong, L., Steven, G. (2000). Vibration-based model-dependent damage (delamination) identification and health monitoring for composite structures — a review. *Journal of Sound and Vibration, 230(2),* 357–378. DOI 10.1006/jsvi.1999.2624.
9. Tee, K. F. (2004). *Substructural identification with incomplete measurement for structural damage assessment (Ph.D. Thesis)*. National University of Singapore.
10. Doebling, S. W., Farrar, C. R., Prime, M. B., Shevitz, D. W. (1996). Damage identification and health monitoring of structural and mechanical systems from changes in their vibration characteristics: a literature review. Los Alamos National Laboratory, *Report No. LA-13070-MS*.
11. Farrar, C., Baker, W., Bell, T., Cone, K., Darling, T. et al. (1994). Dynamic characterization and damage detection in the I-40 bridge over the Rio Grande. Los Alamos National Laboratory, *Report LA-12767-MS*.
12. Tee, K. F., Koh, C. G., Quek, S. T. (2004). Substructural system identification and damage estimation by OKID/ERA. *Proceedings of the 3rd Asian-Pacific Symposium on Structural Reliability and its Applications, Seoul,* 637–647.
13. Ajay, K., John, S., Herszberg, I. (2008). Strain-based structural health monitoring of complex composite structures. *Structural Health Monitoring: An International Journal, 7(3),* 203–213. DOI 10.1177/1475921708090559.
14. Siegert, D., Multon, S., Toutlemonde, F. (2005). Resonant frequencies monitoring of alkali aggregate reaction damaged concrete beams. *Experimental Techniques, 29(6),* 37–40. DOI 10.1111/j.1747-1567.2005.tb00245.x.
15. Chen, H. P., Tee, K. F., Ni, Y. Q. (2012). Mode shape expansion with consideration of analytical modelling errors and modal measurement uncertainty. *Smart Structures and Systems, 10(4-5),* 485–499. DOI 10.12989/sss.2012.10.4_5.485.
16. Rytter, A., Krawczuk, M., Kirkegaard, P. (2000). Experimental and numerical study of damaged cantilever. *Journal of Engineering Mechanics, 126(1),* 60–65. DOI 10.1061/(ASCE)0733-9399(2000)126:1(60).
17. Castellini, P., Martarelli, M., Tomasini, E. P. (2006). Laser doppler vibrometry: development of advanced solutions answering to technology's needs. *Mechanical Systems and Signal Processing, 20(6),* 1265–1285. DOI 10.1016/j.ymssp.2005.11.015.
18. Wang, T., Zhang, L., Tee, K. F. (2011). Extraction of real modes and physical matrices from modal testing. *Earthquake Engineering and Engineering Vibration, 10(2),* 219–227. DOI 10.1007/s11803-011-0060-6.
19. Mottershead, J. E., Friswell, M. I. (1993). Model updating in structural dynamics: a survey. *Journal of Sound and Vibration, 167(3),* 347–375. DOI 10.1006/jsvi.1993.1340.
20. Tee, K. F., Cai, Y., Chen, H. P. (2013). Structural damage detection using quantile regression. *Journal of Civil Structural Health Monitoring, 3(1),* 19–31. DOI 10.1007/s13349-012-0030-3.
21. Esfandiari, A., Bakhtiari-Nejad, F., Sanayei, M., Rahai, A. (2010). Structural finite element model updating using transfer function data. *Computers & Structures, 88(1-2),* 54–64. DOI 10.1016/j.compstruc.2009.09.004.

22. Natke, H. G. (1988). Updating computational models in the frequency domain based on measured data: a survey. *Probabilistic Engineering Mechanics, 3(1),* 28–35. DOI 10.1016/0266-8920(88)90005-7.
23. Friswell, M. I., Penny, J. E. T. (1990). Updating model parameters from frequency domain data via reduced order models. *Mechanical Systems and Signal Processing, 4(5),* 377–391. DOI 10.1016/0888-3270(90)90064-R.
24. Modak, S. V., Kundra, T. K., Nakra, B. C. (2002). Comparative study of model updating methods using simulated experimental data. *Computers & Structures, 80(5-6),* 437–447. DOI 10.1016/S0045-7949(02)00017-2.
25. Klepka, A., Staszewski, W. J., DiMaio, D., Scarpa, F., Tee, K. F. et al. (2013). Sensor location analysis in nonlinear acoustics used for damage detection in composite chiral sandwich panels. *Advances in Science and Technology, 83,* 223–231. DOI 10.4028/www.scientific.net/AST.83.223.